

Detection of Al³⁺ by fluorescent turn-on nitrogen/sulphur-binary doped carbon dots

Siti Raudhatul Kamali¹, Chang-Nan Chen²★, and Tai-Huei Wei³

¹Department of Environmental Science, University of Mataram, Mataram 83125, Indonesia

²Department of Applied Chemistry, Chaoyang University of Technology, Taichung 413310, Taiwan

³Department of Physics, National Chung Cheng University 621301, Chiayi, Taiwan

(Received March 2, 2023; Revised April 4, 2023; Accepted April 10, 2023)

Abstract: In this study, a straightforward and precise nitrogen/sulphur-codoped carbon dots (N/S-CD) was produced using a microwave irradiation approach. The N/S-CD was formulated from succinic acid (SA), bis-(3-aminopropyl)-amine (BAPA), and sodium thiosulphate (STS) as sources of carbon, nitrogen, and sulphur, respectively. The synthesized N/S-CD established a valuable quantum yield (QY) of 70 % and was sensitive to aluminium ion (Al³⁺) with a detection limit of 0.21 μM and a linear concentration range of 0-100 μM. When detecting Al³⁺ in real water samples, the N/S-CD resulted in a satisfactory recovery in the range of 91.14 %-103.37 %. Thus, the proposed study is very promising for Al³⁺ detection in environmental water samples.

Key words: carbon dots, microwave, aluminium ion, water samples

1. Introduction

The element of aluminum is the third largest on earth. Although it is a non-essential element, excess levels of Al in the human body can cause a variety of diseases, including amyotrophic lateral sclerosis, dialysis-induced encephalopathy, Parkinson's disease, and Alzheimer's disease.¹ A combination of factors contribute to the biomagnification of Al in the human body, including contamination in drinking water, food, and bioaccumulation by plants and animals.² Consequently, the need for a detection method for Al in the environment becomes extremely urgent in the near future.

It has been proven in recent years that some analytical instruments can be used for the detection of Al³⁺, including the atomic absorption spectroscopy (AAS),³ inductively coupled plasma (ICP).⁴ However, these instruments are expensive and complicated in analysis. Therefore, it is required to develop a simple and inexpensive Al ion detection method, such as carbon dots (CDs).

Nowadays, CDs are the focus of attention of several researchers to monitor various analytes, both organic and inorganic because of their low cost, easy operation, good selectivity and sensitivity.⁵ However, the relatively low of quantum yield (QY) as well as low selectivity and sensitivity are one of the limitations of CDs as a

★ Corresponding author

Phone : +886-4-23323000, Fax : +886-4-23329898

E-mail : cnchen@cyut.edu.tw

This is an open access article distributed under the terms of the Creative Commons Attribution Non-Commercial License (<http://creativecommons.org/licenses/by-nc/3.0>) which permits unrestricted non-commercial use, distribution, and reproduction in any medium, provided the original work is properly cited.

fluorescence probe. Doping CDs with elements such as N, P, B, and S is a straightforward and useful technique for increasing fluorescence efficiency.⁶ Generally, doping with two heteroatoms is more efficient than doping with a single heteroatoms.⁷ Nitrogen and sulphur are two atoms that are similar to carbon atom in terms of their atomic radius and electronegativity, so nitrogen and sulphur are often studied as carbon doping or co-doping of CDs.⁸

In this work, we establish a novel fluorescence nitrogen/sulphur co-doped carbon dots (N/S-CD) synthesized via an easy and cost-effective microwave irradiation approach by introducing succinic acid (SA), sodium thiosulphate (STS), and bis-(3-aminopropyl)-amine (BAPA) as carbon, nitrogen, and sulphur sources, respectively, for detecting Al^{3+} . Many synthetic methods have been reported to produce CDs using high-purity chemicals, but no study has revealed N/S-CD synthesis using the microwave method to detect Al^{3+} . Due to the simplicity, fast, cost-effectiveness, and environmentally-friendly, the microwave method is one of the most bottom-up methods for preparing of CDs.⁹

A preliminary study showed that SA-based CDs with no additional atomic doping did not exhibit any fluorescent properties during the synthesis process. A new dopant known as BAPA is an interesting new dopant that has not yet been studied in terms of improving CDs' optical properties. While the STS compound consists of sulphur (S) which was used to enhance the optical properties of CDs because of its electronegativity comparable to that of carbon.¹⁰ Therefore, the combination of SA with the presence of nitrogen and sulphur binary elements as doping CDs is expected to increase the quantum yield which has implications for increasing the effectiveness of its application.

2. Experimental

2.1. Chemicals and reagents

Succinic acid ($\text{C}_4\text{H}_6\text{O}_4$), bis-(3-aminopropyl)-amine ($\text{HN}[(\text{CH}_2)_3\text{NH}_2]_2$), and quinine sulphate ($\text{C}_{40}\text{H}_{52}\text{N}_4\text{O}_9\text{S}$) were purchased from Sigma-Aldrich (USA). Sodium

thiosulphate ($\text{Na}_2\text{S}_2\text{O}_3$) was procured from Shimakyu's pure chemicals (Japan). Other chemicals were of analytical grade.

2.2. Instrumental

With an accelerating voltage of 200 kV, JEOL JEM-2010 transmission electron microscopy (Japan) was adapted for characterizing of the size and morphology of N/S-CD. To further investigate the elemental analysis of N/S-CD, X-ray photoelectron spectroscopy (XPS) on a PHI Hybrid Quantera was used. The functional group on the surface of the N/S-CD was confirmed by using a Fourier Transform Infrared (FTIR) spectrometer provided by Perkin Elmer (USA). A Lambda Perkin Elmer ultraviolet-visible (UV-Vis) instrument was used to assess the absorption spectra of the samples. The PL intensity of N/S-CD was performed by a fluorescence spectrophotometer (Jasco FP-750, Japan).

2.3. Synthesis of N/S-CD

N/S-CD was fabricated using a simple microwave irradiation approach. Briefly, 0.50 g of SA, 0.35 g of STS and 1 mL of BAPA were dispersed in 15.0 mL of deionized water (DI water). For 5 min, a mixture solution was irradiated with a domestic microwave at 700 W. Following centrifugation of the material at 5,000 rpm for 30 minutes, the material was filtered using a cylindrical membrane filter (0.22 μm) in order to remove the insoluble particles. In the final step, the purified solution was freeze-dried and stored at a temperature of 4 °C for a subsequent analysis.

2.4. Measurement of QY

The QY calculation of N/S-CD refers to the QY equation based on eq. below.

$$QY_n = QY_r \frac{I_n A_r \eta_n^2}{I_r A_n \eta_r^2}$$

As indicated above, subscripts "n" and "r" represent N/S-CD and quinine sulphate, respectively. "I" and "A" are the symbols that indicate the intensity of the PL and the absorbance at the chosen excitation wavelength. Symbol " η " stands for the refractive index of the

solvent. Due to the stability luminescent of quinine sulphate with QY of 0.54, it was preferred to be used as a reference. Furthermore, the PL emission measurements were carried out at a wavelength of 340 nm, which was the maximum excitation wavelength.

2.5. Selectivity and selectivity of Al³⁺

As a part of the evaluation of selectivity, several ions including Al³⁺, Ni²⁺, Cs⁺, K⁺, Li⁺, Mn²⁺, Na⁺, Rb⁺, Hg²⁺, Cr³⁺, Pb²⁺, Ag⁺, Mg²⁺, Zn²⁺, CO₃²⁻, PO₄³⁻, Cu²⁺, and Fe²⁺ were highly diluted in 10 μ L N/S-CD (0.03 mg/mL). Each of the ions had a concentration of 200 μ M.

Moreover, the sensitivity of Al³⁺ ions was evaluated in the presence of various concentrations of Al³⁺, ranging from 0-200 μ M. Following the addition of DI water, the solution was allowed to react for 5 minutes. All treatments were performed in triplicate and PL spectrum was recorded at 340 nm as the excitation wavelength.

2.6. Real water sample applications

To test the effectiveness of N/S-CD (0.03 mg/mL) for practical use in natural conditions, two samples of water (river water and tap water) were treated with N/S-CD (0.03 mg/mL). The water sample was filtered using a 0.22 μ m syringe filter to ensure that

any remaining material could be removed from the water sample. A known concentration of Al³⁺ was spiked into each sample, as well as 10 μ L N/S-CD. At room temperature, all treatments were performed in triplicate.

3. Results and Discussion

3.1. N/S-CD Characterization

The synthesis of N/S-CD by means of microwave irradiation was performed by combining SA as a precursor with STS as a sulphur source and BAPA as a nitrogen source. In terms of solubility in water, the N/S-CD synthesized has a good level of solubility. Based on the plot of integrated PL intensity against the N/S-CD absorbance and quinine sulphate, the QY for N/S-CD has been achieved at 70 %.

TEM image of synthesized N/S-CD was displayed in Fig. 1(a). According to the results, the N/S-CD had spherical shapes and ranged in size from 4-12 nm. As a result of FTIR spectroscopy (Fig. 1(b)), the N/S-CD functional groups were identified.

An absorption peak at 1109 cm⁻¹ corresponds to C-O stretching vibration.¹¹ The characteristic absorption peaks at 1154 cm⁻¹ and 1550 cm⁻¹ may ascribed to C-S/SO₃ and C=N, which indicated the presence of sulphur and nitrogen on the surface of N/S-CD.^{12,13} An absorption peak at 1412 cm⁻¹ was ascribed to

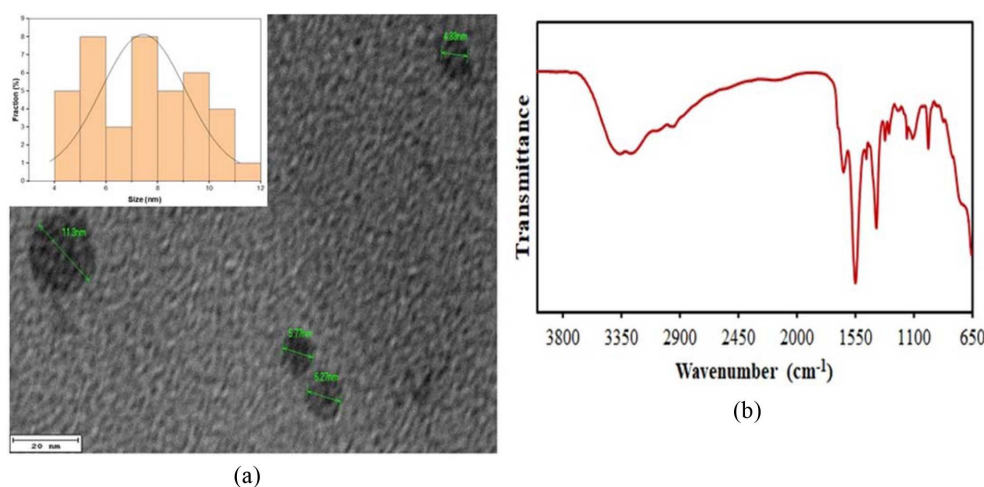


Fig. 1. (a) N/S-CD TEM image, (b) FTIR spectrum of the N/S-CD

C=C stretching vibration.^{11,13} Furthermore, the characteristic peak at 1643 cm^{-1} related to C=O stretching vibration.^{11,14} The peaks at 3431 cm^{-1} , 3264 cm^{-1} , and 2957 cm^{-1} associated with N-H, O-H, and C-H stretching vibration, respectively.¹³ The results of the FTIR analysis have therefore provided proof that there are functional groups of nitrogen and sulfur on the surface of the N/S-CD.

The XPS spectrum shown (Fig. 2(a)) revealed that N/S-CD consists of elements C, O, N and S which were manifested in four peaks as C1s, O1s, N1s, and S2p. The ratio of these elements were 69.4 %, 14.3 %, 14.7 % and 1.6 %. The high-resolution XPS spectra showed the C1s spectrum was deconvoluted into four peaks at 284.8 eV, 285.8, 286.4 and 287.6 eV. As shown in Fig. 2(b), a peak of 284.5 eV was assigned to C=C and subsequent peaks at 285.4, 286.5, and 287.4 eV were assigned to C-C, C-N, and C-S, respectively.¹⁵⁻¹⁷ Fig. 2(c) displayed the high-resolution spectra of O1s consisting two prominent peaks at 531.3 and 532.9 eV, which were ascribed to C=O and C-O groups, respectively.^{16,18} The N1s XPS spectrum of N/S-CD was deconvoluted into three

peaks (Fig. 2(d)), which were corresponded to C-N-C (398.8 eV), N-H (399.5 eV) and C₃-N (400.5 eV).^{18,19} The S2p spectrum (Fig. 2(e)) confirmed two main peaks, which manifested the presence of sulphur in two groups of -C-S- and -C-SO_x-, respectively. The first main peaks at 161.6 and 164.0 eV can be attributed with 2p_{3/2} and 2p_{1/2} of the -C-S- covalent bond.^{15,20} The second main peaks was fitted into three peaks at 167.5, 168.2, and 168.7 eV confirming the presence of -C-SO_x- (x = 2, 3, 4) species.^{20,21}

Accordingly, FTIR and XPS results validated the existence of functional groups including C-N, C-S/C-SO_x, C=C, C=O, -COOH, and -OH on the surface of N/S-CD synthesis.

3.3. Optical properties

Fig. 3 illustrates N/S-CD exhibited UV-Vis absorption spectra in aqueous solution, which showed a peak at 216 nm, followed by a shoulder peak at 264 nm in the UV region. These peak correspond to the π - π^* transition of C=C/C=N.^{20,22} A weak shoulder absorption peak also appear at 340 nm related to n - π^*

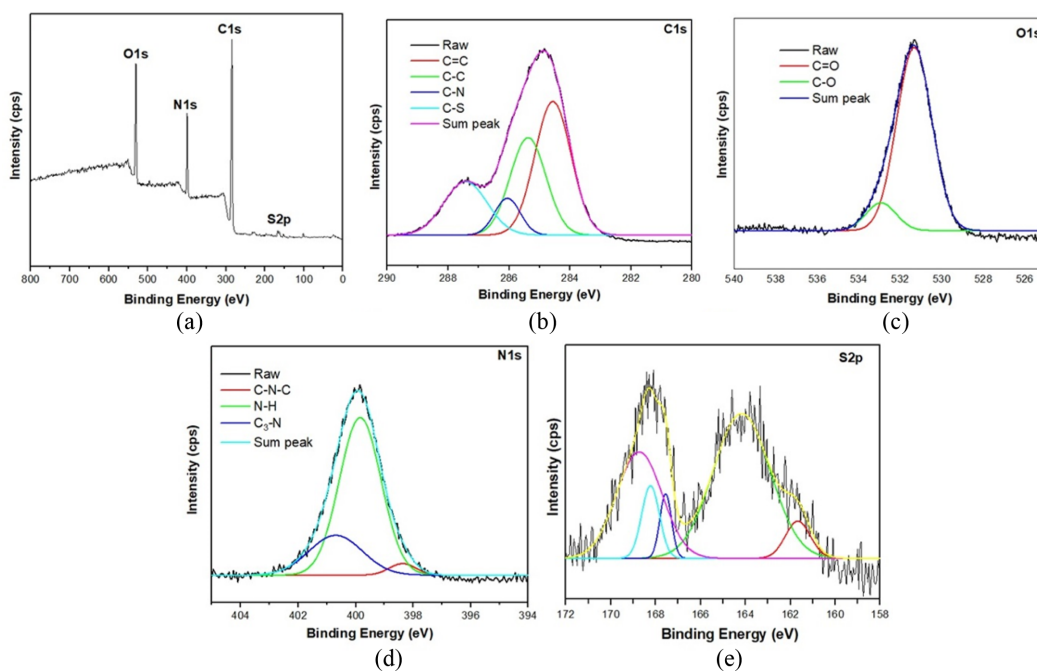


Fig. 2. (a) N/S-CD XPS spectrum. High resolution of XPS spectrum for (b) C1s, (c) O1s, (d) N1s, and (e) S2p.

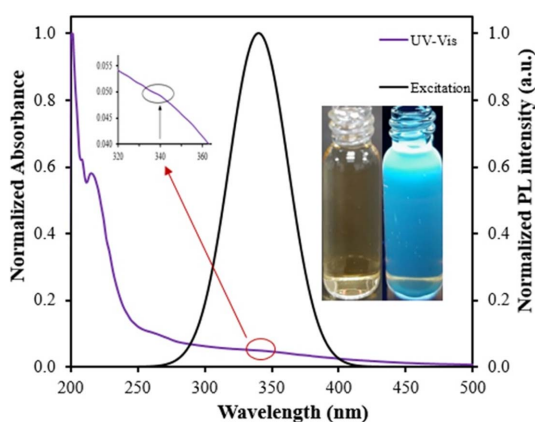


Fig. 3. UV-Vis absorption corresponding to excitation at 340 nm (inset: UV and daylight photographs of N/S-CD).

transition by oxygen or nitrogen functional group on the surface of N/S-CD.^{23,24} The characteristics of N/S-CD are consistent with the general CDs characteristic.⁸

In addition, under exposure to a UV lamp radiation with a 365 nm wavelength, the N/S-CD solution showed a blue color (inset Fig. 3). When the N/S-CD solution was irradiated at different excitation wave-

length, wavelength-dependent fluorescence emissions were found. A strong emission peak was observed at 412 nm when the N/S-CD was conducted at an excitation wavelength of 340 nm. The emission peak of N/S-CD gets red-shifted, accompanied by the fluorescence intensity decrease gradually when the excitation wavelength increases from 300 to 480 nm. This phenomenon belongs to the dependent emission characteristic because of the non-uniform particle size of N/S-CD and the presence of different surface sites on the surface, which is consistent to the previous literature reports.⁵

3.4. Photostability of N/S-CD

Several potential effects on the stability of N/S-CD were investigated in order to evaluate their stability in terms of NaCl concentration, time exposure to UV light (365 nm), temperature, and pH. As shown in Fig. 4(a), the effect of NaCl concentration on N/S-CD appeared to be independent of ionic strength. The findings of this study indicate that stable fluorescence intensities were achieved when NaCl solutions with varying concentrations between 0 and 200 mM were

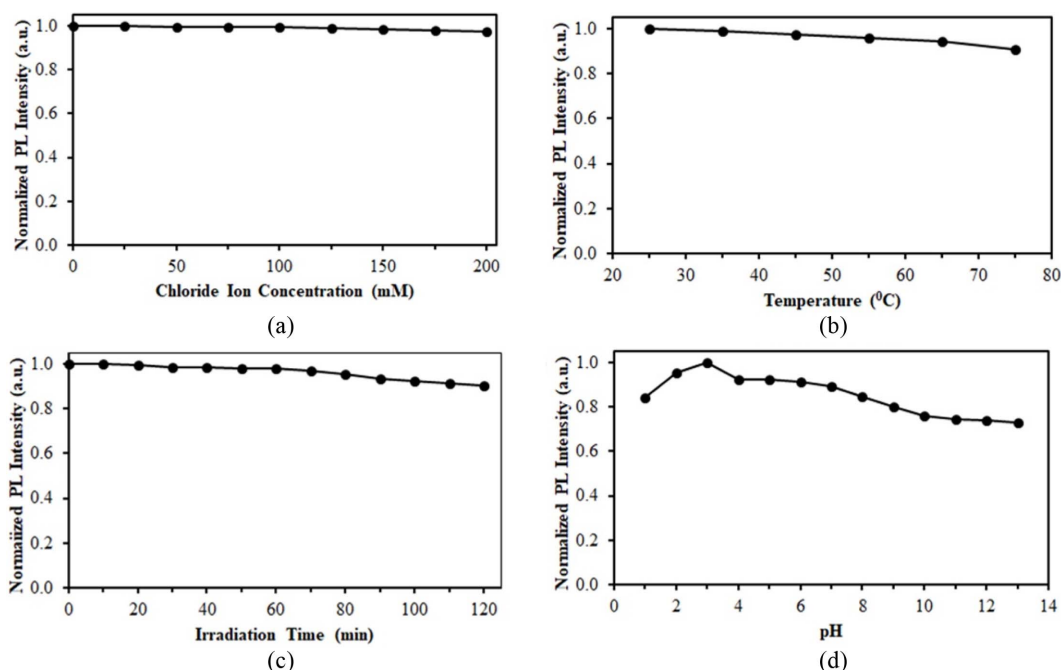


Fig. 4. Stability of N/S-CD: (a) different of chloride ion concentrations, (b) various temperatures, (c) continuous UV irradiation, and (d) various pH.

added to the N/S-CD solution. The fluorescence intensity was almost unchanged even when N/S-CD was injected at high concentrations of NaCl. It was concluded that the N/S-CD solution proved to be very resistant to ionic salts. In other words, N/S-CD has high stability against particle attraction.²²

As opposed to the effect of temperature on the fluorescent intensity, the intensity of the fluorescent decreased with increased temperature (Fig. 4(b)). There was a relationship between non-radiated heat that is produced when the temperature rises, and thus the amount of radiation that was released in the process decreases.

Furthermore, when N/S-CD was irradiated with UV light of 365 nm, it was found that the fluorescence intensity was slightly affected. According to Fig. 4(c), for a given period of time, the fluorescence intensity decreases with lengthening of the irradiation time. PL intensity decreased by 9.8 % after being exposed for 120 minutes to UV irradiation. Compared to the reduction in PL intensity that was observed with traditional fluorescent dyes such as Rhodamine 6G after 120 minutes of continuous exposure, the reduction in PL intensity was almost 54 %, ²⁵ Therefore, N/S-CD will be more resistant to UV radiation than conventional CDs.

In the pH range of 4-7, the fluorescence intensity of N/S-CD appeared to be relatively stable, as depicted in Fig. 4(d). The highest intensity of PL was observed at pH 3. There was a decrease in fluorescence intensity as the pH value increased, which could be attributed to the mechanism of protonation or de-protonation of carboxyl (-COOH) and hydroxyl groups (-OH) on the surface of the N/S-CD.²⁶ As a result, the good stability of N/S-CD provides an invaluable guide in the application of N/S-CD as fluorescent probes that can be used for the detection of metal ions, in particular Al^{3+} , in the environment.²⁷

3.5. Detection of Al^{3+} ion by N/S-CD

For the purpose of evaluating the metal ion sensing capability of fluorescent N/S-CD, 10 μl N/S-CD solution (0.03 mg/mL) was put into glass vials and separately added the relevant metal ions including

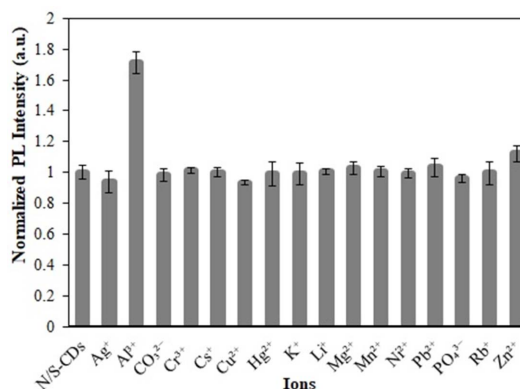


Fig. 5. Detection of Al^{3+} by N/S-CD among various metal ions

Al^{3+} , Cs^+ , K^+ , Li^+ , Mn^{2+} , Na^+ , Rb^+ , Hg^{2+} , Se^{4+} , Ni^{2+} , Pb^{2+} and Fe^{3+} with a concentration of 200 μM . Then, the response of the N/S-CD sensing ability was recorded by fluorescence spectrophotometry.

As shown in Fig. 5, only Al^{3+} ion showed a significant increase in the fluorescence intensity, which indicated the high selectivity of fluorescent N/S-CD towards Al^{3+} ion through the fluorescence “turn-on” process compared to other metal ions.

3.6. Sensitivity of N/S-CD towards Al^{3+}

Further investigation of the advantages above was the measurement of the fluorescence intensity of N/S-CD at various concentrations of Al^{3+} ions. As shown in Figs. 6(a) and 6(b), increasing the concentration of Al^{3+} ions significantly enhanced the emission intensity of N/S-CD. Thus, complex formation was the main probable reason for the increased fluorescence intensity of N/S-CD. A good linear correlation (R^2 , 0.996) was found between Al^{3+} concentration at 0-100 μM and the intensity of fluorescence emission at 412 nm (Inset Fig. 6(b)). Meanwhile, the detection limit for N/S-CD for Al^{3+} was 0.21 μM which was calculated using $3\delta/m$, where a blank signal's standard deviation is indicated by the symbol δ and the slope of the linear correlation is denoted by m .

As shown in Table 1, the performance of the present study was compared with other methods based on CDs, which were also used to detect Al^{3+} ions, including linear detection ranges and detection levels. Compared

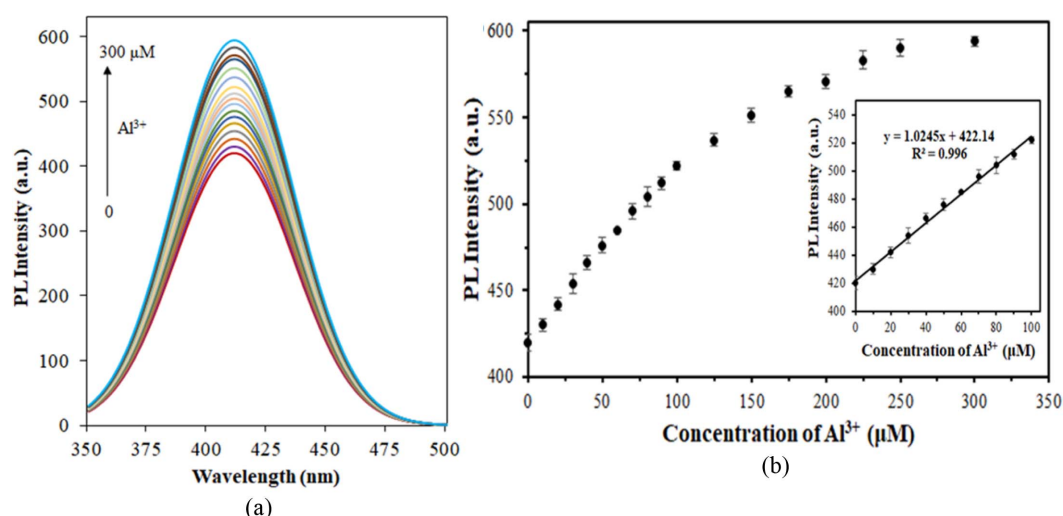


Fig. 6. (a) PL emission spectra of N/S-CD with varying levels of Al³⁺. (b) N/S-CD PL intensity at 412 nm for various Al³⁺ concentrations ranging from 0 to 300 μM (inset: linear curve for Al³⁺ concentrations of 0-100 μM).

Table 1. Review of the various methods for Al³⁺ detection

Method	Linear range (μM)	LOD (μM)	Reference
Nitrogen-doped GQD (N-GQD)	2.5-75	1.3	[29]
CQDs functionalized with amino acids (AA-CQDs)	1-20	0.32	[30]
Amphiphilic fluorescent carbon dots (A-CDs)	8-20	0.113	[31]
Green photoluminescent CDs	0-10	0.39	[32]
Blue emission carbon dots (CDs)	0.15-38.46	0.114	[33]
Nitrogen/sulphur-binary doped carbon dots (N/S-CD)	0-100	0.21	This work

Table 2. Determination of Al³⁺ water samples (n=3)

Sample	Spiked Concentration (μM)	Measured Concentration (μM)	Recovery (%)	RSD (%)
Tap Water	10.00	9.11	91.14	0.57
	20.00	20.67	103.37	0.65
	30.00	28.78	95.92	0.50
River Water	10.00	9.30	93.02	0.46
	20.00	19.10	95.49	0.24
	30.00	30.64	102.13	0.49

to other methods, the probe presented a lower limit of detection (LOD) and a wider range of linear concentrations. The N/S-CD probe also demonstrated that the detection results were below the WHO's remanded value for drinking water of 7.41 μM.^{1,28} These results indicate that the proposed method is quite promising for detecting Al³⁺ ion with an uncomplicated procedure or equipment.

3.7 Detection of Al³⁺ using N/S-CD on water samples

To investigate the feasibility of N/S-CD for Al³⁺ detection, the probes were applied to two water sources treated with known concentrations of Al³⁺. According to Table 2, the percentage recovery of water samples varies in the range of 91.14-103.37. In addition, the results of the relative standard deviation range (RSD)

also showed good results, which ranged from 0.24 to 0.65. Based on these findings, N/S-CD has the potential to be employed as a sensor for detecting Al^{3+} in water under natural environmental conditions.

4. Conclusions

To summarize, using microwave irradiation as a method of synthesizing N/S-CD, we have been able to achieve high quantum yields of the product. A good water solubility was observed for the N/S-CD and its emission properties was excitation-dependent. There was a strong enhancement of fluorescence intensity of N/S-CD in the presence of Al^{3+} . Furthermore, N/S-CD was effectively practiced as a fluorescent sensor to detect Al^{3+} with good selectivity and a wide range of concentrations. This work contributes an effortless and environmentally friendly way to synthesize heteroatom-doped carbon dots for numerous applications.

Acknowledgements

We would like to thank the Department of Applied Chemistry of Chaoyang University of Technology (CYUT), Taiwan. Taking this opportunity, the first author wishes to thank the University of Mataram, Indonesia, for its support in this study.

References

1. L. Bai, Y. Xu, G. Li, S. Tian, L. Li, F. Tao, A. Deng, S. Wang, and L. Wang, *Polymers*, **11**(4), 573 (2019). <https://doi.org/10.3390/polym11040573>
2. M. V. Peto, *Rejuvenation Res.*, **13**(5), 589-598 (2010). <https://doi.org/10.1089/rej.2009.0995>
3. A. Mishra, S. R. Bhalla, S. Rawat, V. Bansal, R. Sehgal, and S. Kumar, *Biologicals*, **35**(4), 277-284 (2007). <https://doi.org/10.1016/j.biologicals.2007.03.003>
4. V. Chrastný and M. Komárek, *Chem. Pap.*, **63**(5), 512-519 (2009). <http://dx.doi.org/10.2478/s11696-009-0057-z>
5. H. Lin, J. Huang, and L. Ding, *J. Nanomater.*, **2019**, 5037243 (2019). <http://dx.doi.org/10.1155/2019/5037243>
6. K. Dehvari, S. H. Chiu, J. S. Lin, W. M. Girma, Y. C. Ling, and J. Y. Chang, *Acta Biomater.*, **114**, 343-357 (2020). <https://doi.org/10.1016/j.actbio.2020.07.022>
7. F. Yuan, Z. Wang, X. Li, Y. Li, Z. Tan, L. Fan, and S. Yang, *Adv. Mater.*, **29**(3), 1604436 (2017). <https://doi.org/10.1002/adma.201604436>
8. Y. Li, Y. Hu, Y. Jia, X. Jiang, and Z. Cheng, *Anal. Lett.*, **52**(11), 1711-1731 (2019). <https://doi.org/10.1080/00032719.2019.1566349>
9. W. L. Ang, C. A. L. B. Mee, N. S. Sambudi, A. W. Mohammad, C. P. Leo, E. Mahmoudi, M. M. Ba-Abbad, and A. Benamor, *Sci. Rep.*, **10**(1), 21199 (2020). <https://www.nature.com/articles/s41598-020-78322-1>
10. A. Saengsrichan, C. Saikate, P. Silasana, P. Khemthong, W. Wanmolee, J. Phanthasri, S. Youngjan, P. Posoknistakul, S. Ratchahat, N. Laosiripojana, K. C. W. Wu, and C. Sakdaronnarong, *Int. J. Mol. Sci.*, **23**(9), 5001 (2022). <https://doi.org/10.3390/ijms23095001>
11. J. Y. Liang, L. Han, S. G. Liu, Y. J. Ju, N. B. Li, and H. Q. Luo, *Spectrochim. Acta A Mol. Biomol. Spectrosc.*, **222**(80), 117260 (2019). <https://doi.org/10.1016/j.saa.2019.117260>
12. R. Bisauriya, S. Antonaroli, M. Ardini, F. Angelucci, A. Ricci, and R. Pizzoferrato, *Sensors*, **22**(7), 2487 (2022). <https://doi.org/10.3390/s22072487>
13. Y. Chen, H. Cui, M. Wang, X. Yang, and S. Pang, *Colloids Surf. A Physicochem. Eng. Asp.*, **638**, 128164 (2021). <https://doi.org/10.1016/j.colsurfa.2021.128164>
14. J. C. Jin, Y. Yu, R. Yan, S. L. Cai, X. Y. Zhang, F. L. Jiang, and Y. Liu, *ACS Appl. Bio Mater.*, **4**(6), 4973-4981 (2021). <https://doi.org/10.1021/acsabm.1c00242>
15. F. Nemat, R. Zare-Dorabei, M. Hosseini, and M. R. Ganjali, *Sens. Actuators B Chem.*, **255**, 2078-2085 (2018). <https://doi.org/10.1016/j.snb.2017.09.009>
16. J. Shen, S. Shang, X. Chen, D. Wang, and Y. Cai, *Sens. Actuators B Chem.*, **248**, 92-100 (2017). <https://doi.org/10.1016/j.snb.2017.03.123>
17. S. Chandra, P. Patra, S. H. Pathan, S. Roy, S. Mitra, A. Layek, R. Bhar, P. Pramanik, and A. Goswami, *J. Mater. Chem. B.*, **1**(18), 2375-2382 (2013). <https://doi.org/10.1039/C3TB00583F>
18. W. U. Khan, D. Wang, W. Zhang, Z. Tang, X. Ma, X. Ding, S. Du, and Y. Wang, *Sci. Rep.*, **7**(1), 14866 (2017). <https://www.nature.com/articles/s41598-017-15054-9>
19. L. Wang, W. M. Choi, J. S. Chung, and S. H. Hur,

- Nanoscale Res. Lett.*, **15**(1), 222 (2020). <https://doi.org/10.1186/s11671-020-03453-3>
20. H. Ding, J. S. Wei, and H. M. Xiong, *Nanoscale*, **6**(22), 13817-13823 (2014). <https://doi.org/10.1039/C4NR04267K>
21. A. Gupta and C. K. Nandi, *Sens. Actuators B Chem.*, **245**, 137-145 (2017). <http://dx.doi.org/10.1016/j.snb.2017.01.145>
22. S. Jayaweera, K. Yin, and J. W. Ng, *J. Fluoresc.*, **29**(6), 221-229 (2019). <https://doi.org/10.1007/s10895-018-2331-3>
23. A. Ghanem, R. Q. B. Al-Marjeh, and Y. Atassi, *Heliyon*, **6**(4), e03750 (2020). <http://dx.doi.org/10.1016/j.heliyon.2020.e03750>
24. S. D. Dsouza, M. Buerkle, P. Brunet, C. Maddi, D. B. Padmanaban, A. Morelli, A. F. Payam, P. Maguire, D. Mariotti, and V. Svrcek, *Carbon*, **183**, 1-11 (2021). <https://doi.org/10.1016/j.carbon.2021.06.088>
25. F. Madjene, M. Assassi, I. Chokri, T. Enteghar, and H. Lebig, *Water Environ. Res.*, **93**(1), 112-122 (2021). <https://doi.org/10.1002/wer.1360>
26. S. Huang, E. Yang, J. Yao, X. Chu, Y. Liu, and Q. Xiao, *Microchim. Acta.*, **186**(12), 851 (2019). <https://doi.org/10.1007/s00604-019-3941-4>
27. M. A. Issa and Z. Z. Abidin, *Molecules*, **25**(15), 3541 (2020). <https://doi.org/10.3390/molecules25153541>
28. T. Han, X. Feng, B. Tong, J. Shi, L. Chen, J. Zhi, and Y. Dong, *Chem. Commun.*, **48**(3), 416-418 (2012). <https://doi.org/10.1039/C1CC15681K>
29. C. Yan, L. Guo, X. Shao, Q. Shu, P. Guan, J. Wang, X. Hu, and C. Wang, *Anal. Bioanal. Chem.*, **413**(21), 3965-3974 (2021). <http://dx.doi.org/10.1007/s00216-021-03348-x>
30. D. Kong, F. Yan, Y. Luo, Q. Ye, S. Zhou, and L. Chen, *Anal. Chim. Acta.*, **953**, 63-70 (2017). <http://dx.doi.org/10.1016/j.aca.2016.11.049>
31. X. Y. Sun, L. L. Wu, J. S. Shen, X. G. Cao, C. Wen, B. Liu, and H. Q. Wang, *RSC Adv.*, **6**, 97346-97351 (2016). <https://doi.org/10.1039/C6RA19370F>
32. W. Wei, J. Huang, W. Gao, X. Lu, and X. Shi, *Chemosensors.*, **9**(2), 25 (2021). <http://dx.doi.org/10.3390/chemosensors9020025>
33. S. Sooksin, V. Promarak, S. Ittisanronnachai, and W. Ngeontae, *Sens. Actuators B Chem.*, **262**, 720-732 (2018). <http://dx.doi.org/10.1016/j.snb.2018.01.239>

Authors' Positions

Siti Raudhatul Kamali : Assistant Professor
Chang-Nan Chen : Assistant Professor
Tai-Huei Wei : Professor